Eur J Plant Pathol (2011) 130:489–502
DOI 10.1007/s10658-011-9768-4

ROS and NO production in compatible and incompatible tomato-*Meloidogyne incognita* interactions

Maria Teresa Melillo · Paola Leonetti · Antonella Leone · Pasqua Veronico · Teresa Bleve-Zacheo

Accepted: 2 March 2011 / Published online: 18 March 2011

Abstract Nitric oxide (NO) has been shown to be an essential regulatory molecule in plant response to pathogen infection in synergy with reactive oxygen species (ROS). At the present, nothing is known about the role of NO in disease resistance to nematode infection. We used a resistant tomato cultivar with different sensitivity to avirulent and virulent populations of the root-knot nematode *Meloidogyne incognita* to investigate the key components involved in oxidative and nitrosative metabolism. We analyzed the superoxide radical production, hydrogen peroxide content, and nitric oxide synthase (NOS)-like and nitrate reductase activities, as potential sources of NO. A rapid NO accumulation and ROS production were found at 12 h after infection in compatible and incompatible tomato-nematode interactions, whereas the amount of NO and ROS gave different results 24 and 48 h after infection amongst compatible and incompatible interactions. NOS-like arginine-dependent enzyme rather than nitrate reductase was the main source of NO production, and NOS-like activity increased substantially in the incompatible interaction. We can envisage a functional overlap of both NO and ROS in tomato defence response to nematode invasion, NO and H_2O_2 cooperating in triggering hypersensitive cell death. Therefore, NO and ROS are key molecules which may help to orchestrate events following nematode challenge, and which may influence the host cellular metabolism.

Keywords Defence response · H_2O_2 · NO · ROS · Root-knot nematodes · Tomato

Abbreviations

cPTIO	2-(4-Carboxyphenyl)-4,4,5,5-tetramethylimidazoline-1-oxyl-3-oxide
DAF-2DA	4,5 diaminofluorescein diacetate
DAPI	4′,6-diamidino-2- phenylindole dihydrochloride
DPI	Diphenylene-iodonium
HPF	2-[6-(4′-hydroxy) phenoxy-3H-xanthen-3-on-9-yl] benzoic acid
Mn-DFA	Mn-desferrioxamine
L-NAME	N^G-nitro-L-Arg methyl ester
$ONOO^-$	Peroxynitrite
SHAM	Salicylhydroxamate
XTT	Na, 3′-{1-[phenylamino-carbonyl]-3,4-tetrazolium}-bis (4-methoxy-6-nitro) benzene-sulfonic acid hydrate

Maria Teresa Melillo and Paola Leonetti contributed equally to this paper.

M. T. Melillo (✉) · P. Leonetti · P. Veronico · T. Bleve-Zacheo
Istituto per la Protezione delle Piante, CNR,
Via Amendola 122/D,
70126 Bari, Italy
e-mail: m.melillo@ba.ipp.cnr.it

A. Leone
Istituto di Scienze delle Produzioni Alimentari, CNR,
Strada Prov.le Lecce-Monteroni,
73100 Lecce, Italy

Introduction

Plants have evolved a variety of defence mechanisms to prevent penetration and growth of pathogens and to induce synthesis of several defence-related compounds such as specific proteins triggering the hypersensitive response (HR) (Jones and Dangl 2006). The timely perception of the invader is central to successful plant defence and involves recognition of elicitors generated or released by pathogens, which in turn stimulate the signalling cascades leading to enhanced resistance. The HR includes the oxidative burst that is characterized by rapid and transient accumulation of reactive oxygen species (ROS), mainly superoxide anion ($O_2^{\cdot-}$) and hydrogen peroxide (H_2O_2) (Apel and Hirt 2004). Hypersensitive cell death, occurring at the infection sites, is regarded as a kind of programmed cell death (PCD) with apoptosis-like features. ROS signalling has been associated and reported to work in concert (Wendehenne et al. 2004; Courtois et al. 2008) with nitric oxide (NO), a highly reactive nitrogen species produced after pathogen and elicitor recognition (Delledonne et al. 2001; Asai et al. 2008). A growing body of evidence indicates that a balance between H_2O_2 and NO is key to determine the fate of cell death (Zeier et al. 2004; Van Breusegem and Dat 2006) and, more, ROS may serve as a secondary message in the establishment of defence (Torres et al. 2006). Biochemical evidence suggests that the immediate downstream of the elicitor-receptor recognition and the production of H_2O_2 represent the initial defence response in plant cells and appear to be mediated through the regulation of plasma membrane-bound enzymes. These include, amongst others, the induction of a plasma membrane-bound NADPH oxidase which mediates the production of H_2O_2 (Sagi and Fluhr 2006), and ROS.

There are several potential pathways that generate endogenous NO in plants and the contribution of each pathway to the overall NO production seems to be dependent upon species, developmental stages, and environment in which plants are grown (Neill et al. 2008). Nitric oxide synthase (NOS)-like and nitrate reductase (NR) are two key enzymes for NO synthesis in plants (Neill et al. 2008). Although great progress has been made in understanding NO biology using model plant-pathogen interactions, few studies have assessed its spatio-temporal role in economically important crop-pathogen interactions (Tada et al. 2004; Requena et al. 2005). No data at all concerning the role of NO in plant-nematode interaction are available to date. In this paper we applied such analyses to tomato roots when challenged by the root-knot nematode *Meloidogyne incognita*.

Root-knot nematodes (RKN) are obligate biotrophic parasites which cause serious losses in a wide range of crops throughout the world. They represent the most advanced type of parasitism by altering gene expression in the host cells which are modified into specialized feeding sites (Abad et al. 2003). Infective second stage juveniles (J2) burrowing into the root establish an intimate relationship within their hosts. Injection of secretions originated from their oesophageal glands induces and maintains a number of multinucleate giant cells which act as metabolic sinks for parasite development. The morphological response of compatible plants to *Meloidogyne* infection is the characteristic root galling, due to hypertrophy of cortical tissue around the giant cells. Specific compound secretions are suggested to bind to plant cell receptors to elicit a signal transduction cascade which modulates gene expression (Bellafiore et al. 2008). As a consequence, altering the uptake of nutrients and water from the plant to the nematode reduces plant growth and crop yield.

Current nematode control includes application of nematicides, crop rotation and introduction of natural resistance traits by conventional breeding, but host resistance is very limited and nematode biotypes "breaking" this resistance are continuously emerging. Numerous genes that confer resistance to RKN have been described, and *Mi* has been found to confer resistance against three species of *Meloidogyne* spp. in tomato (Williamson and Gleason 2003). The incompatible tomato-*Meloidogyne* interaction is characterized by HR and this response is thought to be triggered by direct or indirect interaction of nematode effectors with avirulence activity to corresponding plant resistance gene products. One of the first signs of incompatibility conditioned by *Mi* is a substantial ROS production and H_2O_2 accumulation on plasma membranes and walls of injured cells (Melillo et al. 2006).

The aim of this work was to investigate the role of ROS and NO in the interaction between avirulent (avr) and virulent (vir) *M. incognita* pathotypes, respectively, and resistant tomato.

In order to verify whether NO can act as a signal molecule mediating response to nematode infection

and to evaluate its possible synergistic effect with H_2O_2 in triggering HR in tomato plants, NO level was recorded at different times of infection by means of confocal laser scanning microscope (CLSM) and fluorimetric analyses, and $O_2^{\cdot-}$ and H_2O_2 production was assessed by colorimetric quantification. NO was found to be generated very early in nematode infected roots where H_2O_2 and $O_2^{\cdot-}$ accumulated later, when cell death was evident. Therefore, it could be suggested that the coordinated levels of NO, $O_2^{\cdot-}$, and H_2O_2 are important regulators for HR and are required for plant immune responses.

Materials and methods

Biological material

Two *M. incognita* isolates, avirulent and virulent against the resistant tomato (*Solanum lycopersicum* L.) cv. Rossol carrying the *Mi* gene, were used in the experiments. Five day-old seedlings were inoculated with 125 J2 of either avr- or vir- pathotypes, maintained in a growth chamber at 24±1°C, and watered with Hoagland's solution containing 10 mM KNO_3. At 12, 24, and 48 h after inoculation, plantlets were removed, roots were carefully washed and examined under a stereo microscope.

In planta localization of NO and $ONOO^-$ by CLSM

To analyse NO production by CLSM, Rossol tomato roots, uninfected and infected with avr- and vir- pathotypes (12, 24 and 48 h after inoculation), respectively, were incubated with 10 μM DAF-2DA (Alexis Biochemicals), in 10 mM Tris/KCl, pH 7.2 for 1 h at 25° C in the dark. The roots were washed three times in fresh buffer to remove excessive fluorophore, and examined with CLSM using a dual-channel laser confocal system (LSM Pascal Zeiss) coupled to an Axiover 200 inverted microscope (Zeiss) and equipped with He-Ne and Ar lasers. Dye emission was recorded on 1 μm serial sections using a 490 nm excitation and 505 to 530 nm emission barrier filters. Images were processed and analysed by Zeiss LSM 5 Pascal software version 2.8.

To scavenge NO, roots were pre-treated with 200 μM cPTIO (Alexis Biochemicals) in 10 mM Tris/KCl, pH 7.2, overnight at 25°C, then incubated with DAF-2DA and analysed as above.

The generation of peroxynitrite was detected in uninfected and 24 h avr- pathotype infected roots incubated with 10 μM HPF (Alexis Biochemicals) in 20 mM potassium phosphate buffer pH 7.0 in the dark for 30 min at 25°C and observed at CSLM (490 nm of excitation and 515–545 nm emission).

Determination of NO release

NO detection was carried out using the fluorimetric method and DAF-2DA as fluorescent probe. Portions of uninfected and 12, 24 and 48 h roots infected with avr- and vir- pathotypes, respectively, were excised and 50 mg of tissues were incubated in 1 ml of Ringer solution (145 mM NaCl, 0.5 mM EGTA, 0.5 mM EDTA, 20 mM Hepes, pH 7.6), added with 10 μM DAF-2DA for 1 h at 25°C on a shaker in the dark. The fluorescence of a 50 μl aliquot was measured at 495 nm excitation, 515 nm emission in a Shimadzu fluorescence spectrophotometer (RF-540, Shimadzu Italy, Milan). Aliquots of complete reaction mixture, without plant material, were used as a negative control. In order to study the effects of inhibitors or scavengers on the nematode-induced NO, plants uninfected and avr- infected were pre-treated with 200 μM cPTIO (NO scavenger), 1 mM sodium azide (NR inhibitor) and 1 mM aminoguanidine (AMG, NOS inhibitor), respectively, for 3 h and treated as described above.

Determination of H_2O_2 content

The quantification of H_2O_2 was carried out using an Amplex Red H_2O_2/peroxidase assay kit according to the manufacturer's instructions (Molecular Probes, Inc.). Portions of the uninfected and 12, 24, and 48 h roots infected with avr- and vir- pathotypes, respectively, were excised and 10 mg of tissues were incubated in 1 ml of reaction mixture containing 75 μl of 10 mM Amplex Red and 150 μl of 10 U/ml horseradish peroxidase in 50 mM of sodium phosphate buffer, pH 7.4, for 1 h at 25°C on shaker in the dark. The absorbance was measured at 571 nm with a Beckmann Coulter DU 800 spectrophotometer (Beckman Instruments, Fullerton, CA). The effect of ROS inhibitors on H_2O_2 production was analysed by pre-incubating root tissues, either with 100 μg/ml of catalase or 2 mM SHAM for 2 h at 25°C. The concentration of H_2O_2 in each sample was calculated using a standard curve of known concentrations of pure H_2O_2.

Determination of $O_2^{\cdot-}$ production

The reduction of XTT (Sigma-Aldrich), which produces a soluble formazan, was used to measure $O_2^{\cdot-}$ production. Root portions (10 mg) from uninfected and 12, 24 and 48 h avr- and vir- nematodes infected tomato seedlings were excised and incubated in 1 ml of the reaction mixture containing 500 μM XTT, 20 mM K-phosphate buffer, pH 6.0, in darkness at 25°C for 1 h. Controls, (water plus XTT and reaction mixture without root tissue), were run in parallel to verify any unspecific absorbance. Fifty μl of all samples were read at 470 nm in a spectrophotometer Beckman Coulter DU 800 (Beckman Instr., Fullerton, CA). The inhibition of $O_2^{\cdot-}$ dependent reduction of XTT was determined by 2 h incubation of 24 h avr-infected roots either in 200 μM DPI-HCl [an NAD(P)H oxidase inhibitor] dissolved in dimethylsulfoxide, or in 10 mM Mn-DFA (an $O_2^{\cdot-}$ scavenger) and then transferred to XTT solution for formazan detection. Absorbance was transformed into molar concentration using an extinction coefficient of 2.16×10^4 l mol^{-1} cm^{-1}.

Enzyme assays

NOS-like activity The NOS-like activity in uninfected and nematode-infected root tissues was estimated by citrulline assay method using the Nitric Oxide Synthase Assay Kit (Calbiochem, San Diego). Briefly 300 mg of frozen root tissues were grounded with liquid nitrogen and then resuspended in extraction buffer (250 mM Tris-HCl, pH 7.4, 10 mM EDTA, 10 mM EGTA), centrifuged at 10,000 *g* for 20 min at 4°C, and the supernatants used for NOS determination. The reaction mixture (50 μl) contained 50 mM Tris-HCl, pH 7.4, 6 μM tetrahydrobiopterin, 2 μM FAD, 2 μM flavin mononucleotide, 10 mM NADPH, 0.1 μM calmodulin, 6 mM $CaCl_2$, 0.3 μM (1 μCi) [^{3}H] arginine (Amersham, Italy), and 9 μl tissue extracts (1 μg μl^{-1} protein). After incubation for 30 min at 30°C, the reaction was stopped by adding 400 μl of stop buffer (50 mM HEPES, pH 5.5, 5 mM EDTA). Equilibrated resin (100 μl) was added to the samples and then removed by centrifugation. Flow-through (400 μl) was added to 3 ml of scintillation liquid and the radioactivity was counted (LS 6000, Beckmann). NOS activity was measured as the difference between L-[U-^{14}C] citrulline produced in the complete reaction medium and that produced in medium containing 1 mM L-NAME. Samples were pre-heated at 95°C for 10 min as negative controls, and a commercial neuronal rat cerebellum extract was used as positive control.

NR activity The activity of NR was assayed following the method of Du et al. 2008 with minor modifications. Approximately 50 mg of frozen powdered of uninfected and 12, 24 and 48 h infected roots were homogenized at 0°C with 500 μl of extraction buffer containing 100 mM HEPES-KOH, pH 7.5, 1 mM EDTA, 5 mM DTT, 10% (*v*/*v*) glycerol, 0.1% Triton X-100, 1% polyvinylpyrrolidone, 5 μM Na_2MoO_4, 20 μM FAD, and 100 μl ml^{-1} protein inhibitor cocktail (Sigma). Contents were centrifuged at 15,000 g for 20 min at 4°C. The activity of NR was measured immediately by mixing 200 μl of root tissue extracts with 400 μl of assay buffer containing 100 mM HEPES-KOH, pH 7.5, 5 mM EDTA, 5 mM KNO_3, 0.25 mM NADH. Also, as a negative control, another batch of the NR reaction mixture was added to 50 μl of 30% (*w*/*v*) trichloroacetic acid to denature NR activity. All NR reaction mixtures and negative controls were incubated at 30°C in the dark for 30 min and then stopped by adding 125 μM phenazine methasulfate and 0.5 mM Zn-acetate. The nitrites were determined colorimetrically at 540 nm by adding 1 ml of 1% (*w*/*v*) sulfanilamide in 3 M HCl plus 1 ml 0.02% (*v*/*v*) N-(1-naphthyl)-ethylenediamine in bidistilled water. NR activity was calculated as μmol NO_2^- $h^{-1}mg^{-1}$ protein.

Protein concentrations were determined with a protein assay kit (Bio-Rad Laboratories Inc) using bovine serum albumine (BSA) as a standard.

Determination of nitrate content

Nitrate content was determined according to Leleu and Vuylsteker 2004. Fifty mg of frozen powdered tissues of uninfected and infected tomato roots (12, 24 and 48 h) were added to 1.5 ml of deionised water and shaken 1 h at 45°C. Samples were centrifuged at 15,000 g for 20 min and supernatants were restored at room temperature. Fifty μl of supernatant were added to 200 μl of 5% (*w*/*v*) salicylic acid in

concentrated H_2SO_4 97% (*w*/*v*). After 15 min of incubation at room temperature, 1 ml of 4 N NaOH was added. When the solution came back to room temperature, the optical density was measured at 410 nm. Nitrate content was expressed as μmol NO_3^- g^{-1} FW and calculated according to a standard curve.

Cell death detection

The Evan's blue method was used to test cell viability in uninfected and 12, 24 and 48 h infected tomato roots (Romero-Puertas et al. 2004). Fresh roots (50 mg) were incubated in 2 ml of 0.25% (*w*/*v*) aqueous solution of Evan's blue for 5 h. After several washing with distilled water, dye bound to dead cells was solubilized in 1 ml of 50% (*v*/*v*) methanol and 1.5% (*w*/*v*) sodium dodecyl sulphate at 60°C for 30 min and then quantified at 595 nm. Heating the tissues, 100% of cell death was obtained. In vivo detection of cell death was carried out in 3 h incubated roots with Evan's blue staining and examined under a stereo microscope equipped with a digital camera.

For laddering analysis, DNA samples extracted by cetyl-trimethyl-ammonium bromide method from frozen uninfected and 12 and 24 h avr-infected root tissues were digested with 100 μg/ml DNase-free RNase for 30 min at 37°C, run on 2% agarose gel, and stained with 0.5 μg/ml ethidium bromide.

Nuclear changes were visualized in root tissues fixed in 2% paraformaldehyde and 1.5% glutaraldehyde in 50 mM sodium cacodylate buffer, dehydrated through an ethanol series and embedded in LR White resin (Sigma). Serial semithin sections were cut and mounted on glass slides, stained with 1 mg l^{-1} DAPI in 10 mM Tris-HCl, pH 7.4 for 10 min and then observed at 340–380 nm under a Leica DML epifluorescence microscope, equipped with a digital camera.

Statistical analysis

Values of three time-repeated experiments were expressed as mean ± SE. Data were analysed with Duncan's multiple range test. The differences between the values of uninfected and infected root tissues, at each time point, were considered significant at $P<0.05$ (*) and $P<0.01$ (**).

Results

In planta localization of NO and $ONOO^-$ by CLSM

Real time imaging of NO in living tomato roots challenged by nematodes was followed by using the cell-permeable probe DAF-2DA at CLSM. The DAF-2DA is considered a NO-specific fluorescent dye and would not react with other ROS. Upon its entry into the cells, it is hydrolysed by endogenous esterase to produce DAF-2, which in the presence of NO and O_2 is converted to the green fluorescent triazole derivative DAF-2T (Lum et al. 2002).

The behaviour of infection in both incompatible (tomato-avr pathotype) and compatible interactions (tomato-vir pathotype) was recorded at 12 and 24 h after nematode inoculation (Fig. 1a, b, c, d). The related cellular localization of endogenous NO and $ONOO^-$ after incubation in DAF-2DA and HPF, respectively, was detected by CSLM in at least 12 tomato seedlings for each infection time considered. In all the roots analysed, the production of NO resulted to be very rapid in both avr- and vir- infected roots. Fluorescence intensity reached its maximum in the cortical cells where nematodes were penetrating, 12 h after nematode inoculation (Fig. 1a, e and b, g). The significant increase of NO detected in both incompatible and compatible interactions (Fig. 1e, g) indicated that NO production at 12 h is dependent on the recognition of pathogen invasion. The NO burst was yet highly detectable in the 24 h avr-pathotype infected roots (Fig. 1f), where cortical cells, in which nematodes were established, resulted to be greatly fluorescent (Fig. 1b, f).

In the 24 h infected cells in the compatible interaction, NO production was mainly located either in the cortical cells or associated with parenchyma cells selected as feeding sites by nematodes (Fig. 1d, h). In particular, the parenchyma cells selected as feeding sites (giant cells) were highly fluorescent (Fig. 1h). NO fluorescence appeared located in the cytoplasm and cell walls (Fig. 1i). In 48 h-infected roots NO production significantly decreased in both compatible and incompatible interactions (not shown). In uninfected tomato roots the basal NO was revealed in rhizodermis and cortical cells (Fig. 1j). Pre-incubation of 12 h avr-infected roots with 200 μm cPTIO (a NO scavenger) induced a strong reduction of NO fluorescence (Fig. 1k).

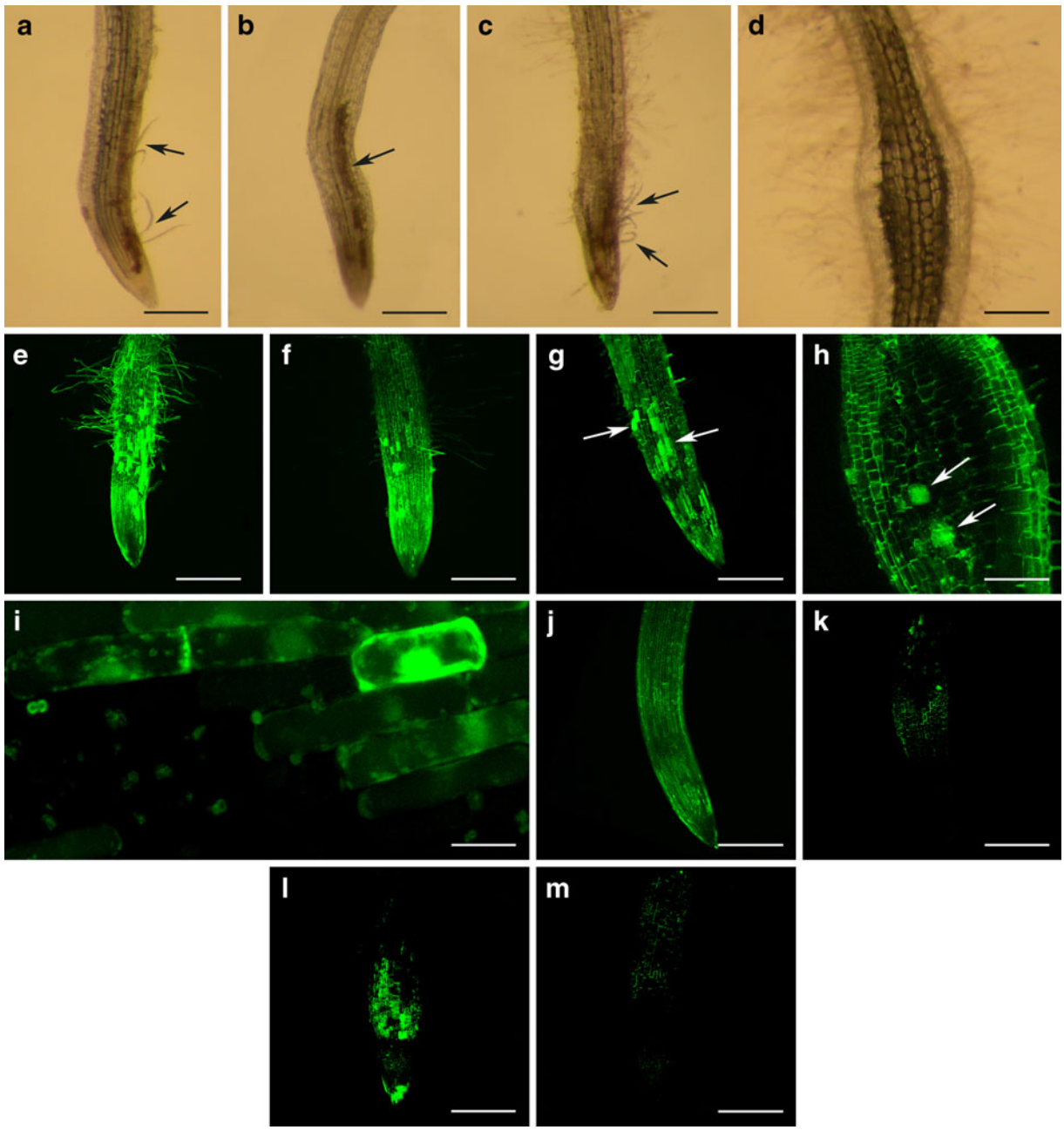

Fig. 1 In vivo images of nematode penetration and NO and $ONOO^-$ detection in tomato roots under light microscope. **a** Browning of cells challenged by avirulent and **c** virulent J2 penetration in tomato root tips at 12 h (*arrows*); **b** HR in 24 h avr-infected root cells (*arrow*) where nematodes were established; **d** a galling 24 h vir-pathotype infected root; **e** great fluorescence detected by CLSM showing NO production induced by nematode penetration in cortical cells as well as in root hairs in a 12 h avr-infected root; **f** spots of green fluorescence in cortical cells of a 24 h avr-infected root, where nematodes were entered; **g** bright fluorescence is visible in injured cortical cells (*arrows*) in a 12 h vir-infected root and **h** is diffuse in cortical cells in a 24 h galling root where two big spots of NO accumulation in developing giant cells (*arrows*) can be seen; **i** detail of NO accumulation in walls, cytoplasm, and nuclei of cortical cells; **j** endogenous NO production in uninfected root; **k** cPTIO strongly reduces NO fluorescence in the avr-infected root; **l** HPF reacts with $ONOO^-$ production in a 24 h avr-nematode infected root and **m** gives a faint fluorescence in uninfected root. Each picture was prepared from 20 to 30 root cross-sections which were analysed by CSLM. Scale bar of all figures=200 μm, except for **d** bar=150 μm, **h** bar=75 μm, and **i** bar=5 μm

Concomitant with the highest NO burst, just at sites of invading juveniles, the 12 h injured roots treated with HPF showed a great fluorescence (Fig. 1l). This indicates that NO reacted with the superoxide radical ($O_2^{\cdot-}$) generating peroxynitrite ($ONOO^-$), not detectable in uninfected roots (Fig. 1m).

Determination of NO release

To confirm the NO production detected by CLSM, NO was monitored fluorimetrically, in a time-course experiment, using the same fluorescent probe DAF-2DA. An increase in NO accumulation occurred in both incompatible (avr-pathotype) and compatible (vir-pathotype) interactions, compared with uninfected tissues (Fig. 2). The most part of NO burst was recorded in the incompatible interaction, and was about 75% at 12 h, 50% at 24 h and 17% at 48 h over the uninfected control (Fig. 2). In the compatible interaction, a rapid increase of 40% was noticed at 12 h, followed by a lower increment at 24 and 48 h compared to the uninfected root tissues (Fig. 2). When samples were pre-incubated with the NO scavenger cPTIO, DAF-2DA dependent fluorescence was reduced about 60%. Moreover, pre-incubation with either AMG (NOS inhibitor) or sodium azide (NR inhibitor) lowered NO production of 90% and 50%, respectively (Table 1).

Table 1 Effect of scavengers and inhibitors on NO (in 12 h Rossol roots infected with avr-pathotype), and H_2O_2 and $O_2^{\cdot-}$ (in 24 h Rossol roots infected with avr-pathotype) production. Data are mean values of three independent experiments ± SE

Treatment	NO production (%)	H_2O_2 production (%)	$O_2^{\cdot-}$ production (%)
None	100±0.1	–	–
+ cPTIO (200 μM)	38±1	–	–
+ AMG (1 mM)	8±0.9	–	–
+ NaN_3 (1 mM)	48±0.3	–	–
None	–	100±1	–
+ Cat (100 μg/ml)	–	19±0.54	–
+ SHAM (2 mM)	–	29±2	–
None	–	–	100±0.2
+ DPI (200 μM)	–	–	10±0.63
+ Mn-DFA (10 mM)	–	–	13±0.84

Determination of H_2O_2 content

Hydrogen peroxide levels were measured by Amplex Red reagent, a specific and sensitive method for extracellular H_2O_2 detection, in uninfected and avr- and vir-pathotype infected root tissues, respectively. The trend of H_2O_2 production resulted to be linear in uninfected root tissues (Fig. 3). Infection with avr- and vir- pathotypes induced a rapid accumulation of H_2O_2 in 12 h injured roots. At 24 and 48 h the production of

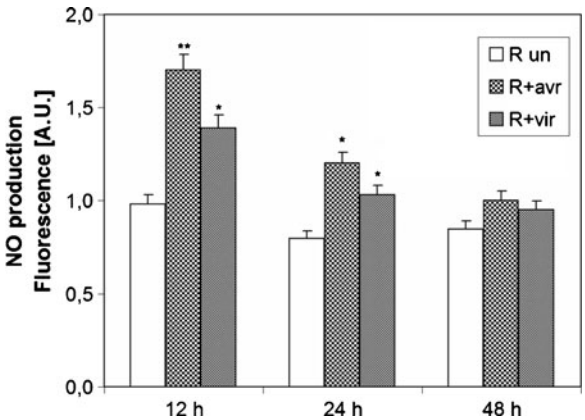

Fig. 2 NO production in tomato Rossol (*R*) uninfected (*un*) and 12, 24 and 48 h infected roots with avirulent (*avr*) and virulent (*vir*) RKN-pathotype, respectively, measured by monitoring DAF-2DA fluorescence. Statistical significance of the differences between uninfected and infected tissues at each time point was determined by Duncan's multiple range test [$P<0.05$ (*) and $P<0.01$ (**)]

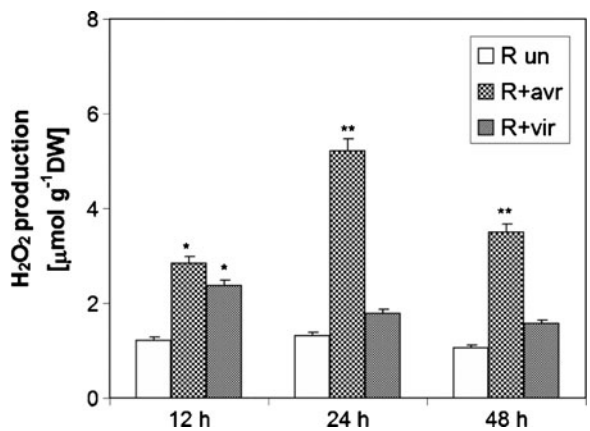

Fig. 3 H_2O_2 concentration in tomato Rossol uninfected and 12, 24 and 48 h infected roots with avr- and vir- pathotype, respectively, using Amplex Red H_2O_2/Peroxidase assay kit. Statistical significance of the differences between uninfected and infected tissues at each time point was determined by Duncan's multiple range test [$P<0.05$ (*) and $P<0.01$ (**)]

H_2O_2 increased significantly in avr-infected roots (incompatible interaction), reaching its maximum at 24 h (Fig. 3). In contrast, H_2O_2 levels were remarkably lower in the compatible than in the incompatible interaction and, had a similar trend at 24 and 48 h (Fig. 3).

To examine the nature of the signal, 24 h avr-infected roots, when the most H_2O_2 production was detectable, were incubated either with catalase (an extracellular H_2O_2 scavenger) or with SHAM (a peroxidase inhibitor). Both catalase and SHAM blocked about 80 and 70% of the Amplex Red reaction, respectively (Table 1).

Determination of $O_2^{\cdot-}$ production

To elucidate the possible correlation between apoplastic superoxide production and nematode induced oxidative burst, the generation of $O_2^{\cdot-}$ was tested by XTT formazan production in both uninfected and infected roots. The assay based on the formation of a soluble formazan dye permitted a reliable quantitative photometric determination of $O_2^{\cdot-}$ in vivo. XTT reduction increased rapidly in the incompatible interaction (avr-pathotype) at 12 and 24 h compared to uninfected controls and started to decline 48 h after nematode infection (Fig. 4). The maximum production of $O_2^{\cdot-}$ (twice more than in controls) was detected in 24 h infected roots. In the compatible interaction (vir-pathotype), the slight increase of $O_2^{\cdot-}$ detected at 12 h, significantly decreased at 24 h, and reached its minimum at 48 h (Fig. 4). DPI [NAD(P)H oxidase inhibitor] and Mn-DFA ($O_2^{\cdot-}$ scavenger) significantly inhibited formazan production (90% and 87%, respectively) in 24 h avr-pathotype infected roots (Table 1).

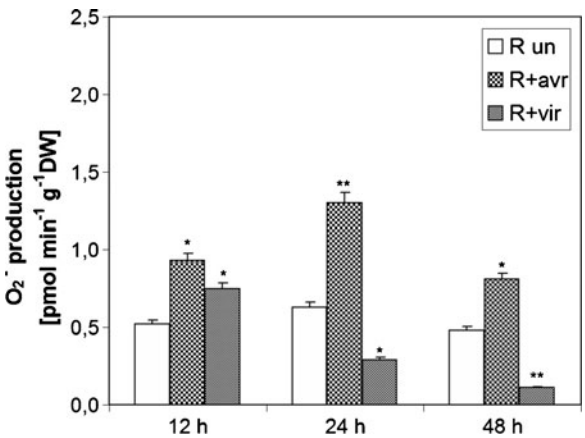

Fig. 4 $O_2^{\cdot-}$ dependent formazan production by XTT in uninfected and 12, 24 and 48 h avr- and vir- infected tomato roots. Statistical significance of the differences between uninfected and infected tissues at each time point was determined by Duncan's multiple range test [$P<0.05$ (*) and $P<0.01$ (**)]

Enzyme assays

NOS-like activity The involvement of a NOS-like enzyme as a source of NO production during nematode infection was considered. The occurrence of NOS-like activity was evaluated as conversion of labelled L-arginine into L-citrulline by tomato root extracts in a time-course experiment in avr- and vir-pathotypes infected and uninfected roots. The difference between the total L-[U-^{14}C] citrulline formation and that inhibited by simultaneous incubation with L-NAME and AMG was used to estimate the NOS-like activity. NOS-like production showed the maximum enzyme activity in 12 h-infected roots in both incompatible and compatible interactions and corresponded to about 15 and 12 pmol L-[U-^{14}C] citrulline $min^{-1}mg^{-1}$prot, respectively, compared to 4 pmol L-[U-^{14}C] citrulline $min^{-1}mg^{-1}$prot founded in uninfected roots (Fig. 5) Enzyme activity gradually declined with the infection time (at 24 and 48 h) in both interactions but its level was always higher (about 8 and 7 pmol, respectively) than in uninfected

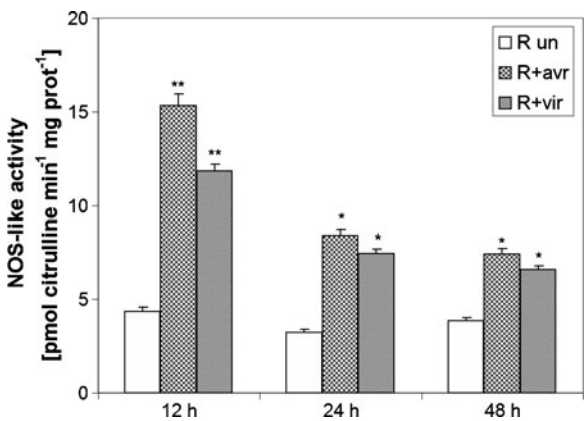

Fig. 5 Analysis of NOS-like activity in uninfected and avr- and vir- nematode infected roots by arginine-citrulline assay method. NOS activity is calculated as the difference between the total L-[U^{14}C] citrulline production and that observed in the presence of cofactors (Ca^{2+} and NADPH) and NOS inhibitor L-NAME (1 mM). Statistical significance of the differences between uninfected and infected tissues at each time point was determined by Duncan's multiple range test [$P<0.05$ (*) and $P<0.01$ (**)]

roots (Fig. 5). NOS-like activity had the same trend of NO production in infected roots.

NR activity NR is the other key enzyme involved in NO synthesis in plants. In our system, NR activity was studied to prove its involvement in endogenous NO production. Unexpectedly, our results showed higher NR activity in uninfected than in infected roots (Fig. 6a). NR activity resulted to maintain the same level in uninfected tissues during the considered times. In infected roots, the NR activity showed its maximum at 12 h and then gradually declined to its minimum at 48 h in both interactions (Fig. 6a). As it is known that the NR activity is bound to uptake of nitrate, NO_3^- concentration in uninfected and nematode infected seedlings, watered with nutrient solution containing 10 mM KNO_3, was measured. The nitrate uptake, found to be quite similar in both uninfected and infected root tissues (about 4 μmoles) at 12 h, was more efficient in uninfected than in infected roots at 24 and 48 h (Fig. 6b). The NO_3^- content started to decline at 24 h, and sharply lowered at 48 h, in both avr- and vir- infected roots (Fig. 6b). These data seem to suggest a relationship between NR activity declining and lowering of nitrate, due, maybe, to the inability of injured tissues (in particular at 24 and 48 h when nematodes have been established) to uptake nitrate sufficiently to sustain NR activity.

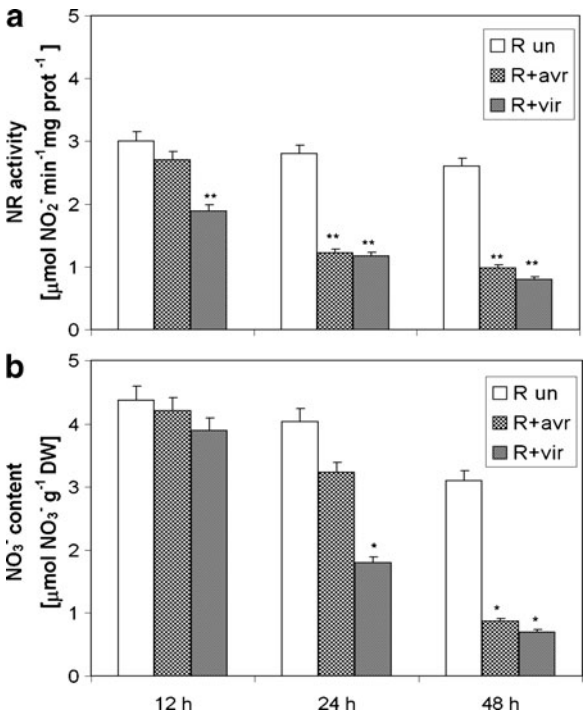

Fig. 6 **a** NR activity in uninfected and avr- and vir- infected tomato roots. NR significantly declines during the infection times **b** determination of nitrate content in uninfected and avr- and vir-infected roots supplied with Hoagland's solution added with 10 mM KNO_3. The trend of nitrates appears to be similar to NR behaviour. Statistical significance of the differences between uninfected and infected tissues at each time point was determined by Duncan's multiple range test [$P<0.05$ (*) and $P<0.01$ (**)]

Cell death detection

The induction of PCD in tomato roots infected with both avr- and vir- pathotypes was studied using different approaches. Staining with Evan's blue dye was used as a marker of cell death in root cells undergoing the HR. Roots incubated with dye and decoloured in methanol showed the most blue staining in cells challenged by avr-pathotype (Fig. 7b, c, d). Cells in 24 h avr-infected roots showed a higher capacity to fix the dye (Fig.7c) than those in vir-infected roots, where the few spots of blue staining observed at 12 and 24 h (Fig. 7e, f) disappeared at 48 h (Fig. 7g). Uninfected roots were completely unstained (Fig. 7a). Colorimetric measurement of Evan's blue dye extracted from roots revealed an increase of cell death of about 25% in 24 h and 48 h avr-infected roots compared to uninfected and vir-infected roots, respectively (Fig. 8). These results seem to suggest a local loss of cell integrity and related cell death following nematode injury.

The analysis of DNA fragment ladders (by agarose gel and ethidium bromide staining), revealing faint bands in avr-infected root samples, was indicative of a great number of cells undergoing to HR in contrast to few cells undergoing to apoptosis (data non shown). Nuclear morphological changes and DNA fragments in infected roots analysed by fluorescence microscopy following DAPI staining confirmed these observations.

Serial longitudinal-sections of a number of uninfected (10) and early stage-infected (20) roots were examined. Nuclei in uninfected roots were usually round or oval in shape and with uniformly granular appearance (Fig. 9a, b). In 12 h vir-infected roots (compatible interaction) few nuclei were lobe-shaped with condensed chromatin (Fig. 9c, d). At 24 h, nuclei maintained more or less the same feature (data not shown). The incompatible response induced morphological changes of nuclei with

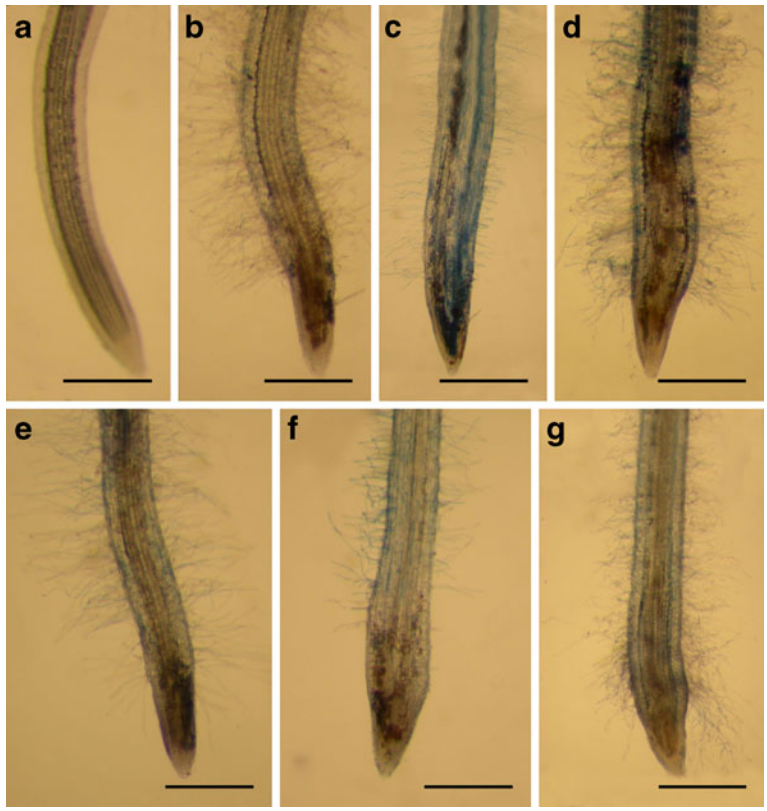

Fig. 7 Analysis of root cell death induction by avr- and vir- pathotype infection. **a** Completely unstained cells by Evan's blue dye in uninfected root; **b** cells blue stained in 12 h avr-, and **e** vir- infected root tip; **c** strongly blue stained cortical cells in 24 h, and **d** 48 h avr-infected roots; **f** blue spots indicate where nematodes are established in a 24 h vir-infected root, and **g** pale blue can be only observed in the cortical tissue of a 48 h vir-root galling. Scale bar=220 μm

chromatin condensation and cytoplasm shrinkage. In 12 h avr-infected roots nuclei in cortical cells challenged by nematode penetration, were flattened and invaginated and their condensed chromatin was visible as bright spots (Fig. 9e, f). In 24 h avr-infected roots, where the nematode was established, nuclei in cells directly injured by J2 and undergoing to HR showed faint fluorescence and were condensed and distorted, whereas some nuclei of adjoining cortical cells showed chromatin fragmentation (Fig. 9g, h). These observations are consistent with those seen in the Evan's blue-stained roots, and would suggest that a necrosis-like cell death is linked to the high presence of ROS and NO.

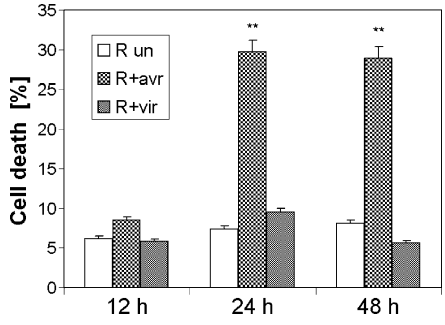

Fig. 8 Time course of cell death in uninfected and infected roots by means of Evan's blue assay measured spectrophotometrically. The percentage of death cells was determined with respect to control. Differences were significant at $P<0.05$ (*) and $P<0.01$ (**) according to Duncan's multiple range test

Discussion

Rapid production of ROS and NO has been reported to play a role in the development and physiological processes, such as in defence responses to biotic or abiotic stresses in plants (Delledonne et al. 2001; Neill et al. 2008).

Previous studies demonstrated that the first 24 h in plant-nematode interaction are critical for determining the plant response to avirulent or virulent *M. incognita*. In general the initial reaction of a susceptible cultivar is similar to that of a resistant host and ROS production can be detected at 12 h after infection during J2 penetration in both cultivars. In the later stages (24 and 48 h) the trend of ROS production became similar in both avr-

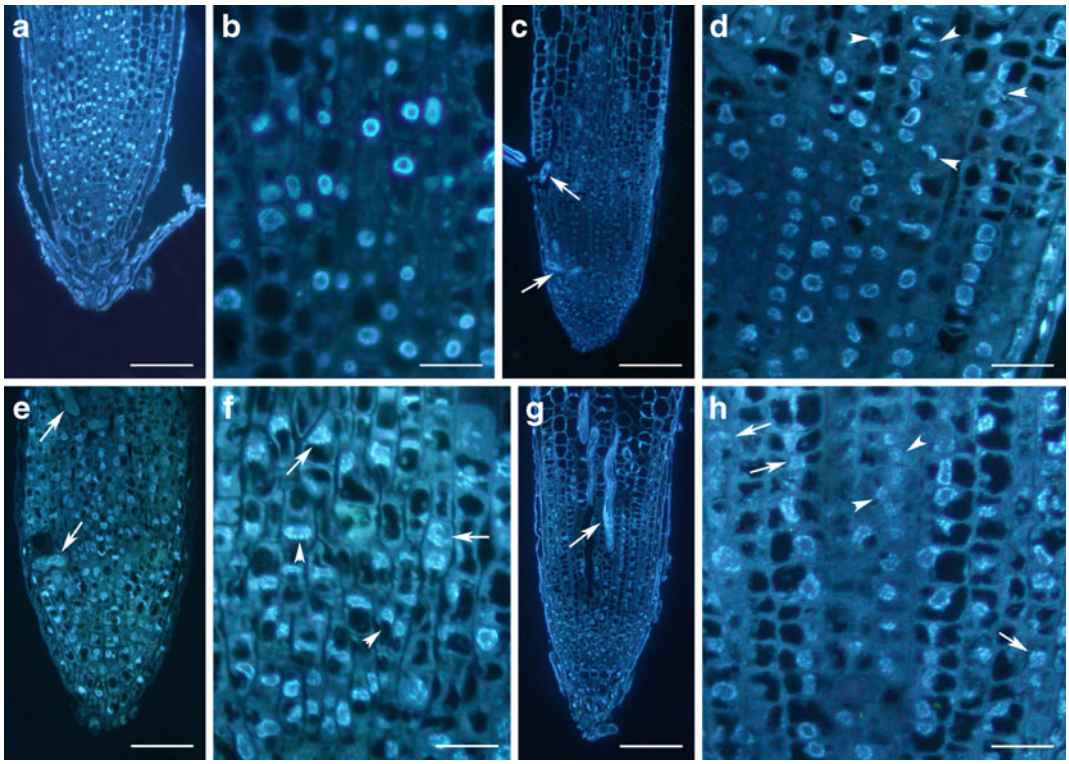

Fig. 9 Nuclear morphology detected by DAPI in avr- and vir-infected tomato roots. **a** DAPI-stained longitudinal section through an uninfected tomato root tip. Bar=100 μm; **b** enlargement of section in **a** showing round and oval shaped nuclei with a normal granular appearance and dispersed chromatin. Bar=25 μm; **c** tangential section of a 12 h-infected root where vir-nematodes are penetrating (*arrows*). Bar=100 μm; **d** enlargement in **c** shows few nuclei with lobed profiles and condensed chromatin (*arrow heads*). Bar=25 μm; **e** nematodes entering in a 12 h avr-infected root (*arrows*). Bar=100 μm; **f** detail of section in **e** reveals flattened and condensed nuclei (*arrow heads*), with spots of brightly stained chromatin (*arrows*). Bar=25 μm; **g** nematodes established in the central cylinder in a 24 h avr-infected root (*arrow*). Bar=100 μm; **h** enlargement of section in **g** shows faint fluorescent nuclei in cells directly injured by nematodes (*arrow heads*) and nuclei with condensed and fragmented chromatin in the adjoining cortical cells (*arrows*). Bar=25 μm

susceptible and in vir-resistant infected cultivars, in concomitance with giant cell induction. This indicates that the vir-pathotype is able to overcome the *Mi* gene and to induce a compatible response (Melillo et al. 2006). Therefore, a resistant tomato challenged by avr- and vir- pathotypes constitutes a good experimental model to follow the morphological and biochemical changes in both incompatible and compatible interactions.

In the present work, there is evidence that both ROS and NO production are increased in tomato roots challenged by avr- and vir- *M. incognita* pathotypes.

The two different techniques used to detect NO (a fluorimetric assay to evaluate NO production at the cellular level and a spectrophotometric assay to quantify NO release by injured tissues) revealed the most increase of NO content as soon as 12 h after nematode inoculation (nematodes need some hours to reach and penetrate into the root tips) and, in particular, in avr-pathotype infected root tissues. DAF-2DA, hydrolysed by cytoplasmic esterases to DAF, reacts with NO in the presence of oxygen to form the highly fluorescent triazolofluorescein. These properties of DAF-2DA and the presence of increased acetyl esterases in tomato cell walls during nematode infection (Melillo et al. 1989) may explain the presence of NO in this subcellular compartment (Fig. 1i). NO accumulation in the cytoplasm and walls of cortical cells had the same feature of ROS production detected by NBT staining (Melillo et al. 2006). This indicates that NO is associated with the HR in the incompatible interaction and, more, can play a role in giant cell development in the compatible relationship, depending on its concentration and relation with ROS.

The sources of NO have been much debated in plants, and two main enzymatic routes, an NO synthase and a nitrate reductase enzymes, have been considered. The L-arginine-dependent pathway is based principally on the assumption that plants do possess nitric oxide synthase (NOS)-like enzyme(s). The presence of NOS activity in plants has been questioned without great success (Crawford et al. 2006). However, several lines of evidence demonstrated the presence of a NOS-like activity in plant cells (Courtois et al. 2008) and, very recently, evidence for the presence of an L-arginine-dependent NOS activity, which is not a canonical animal NOS enzyme, in pea plants, was provided by Corpas et al. (2009). Our results showed that NOS activity increased in both incompatible and compatible interactions and had the same trend of NO production in infected roots.

Several lines of evidence suggested NR as the major source for NO production in plants in response to pathogens or elicitors (Modolo et al. 2006; Yamamoto et al. 2006) and, moreover, the NR pathway was indicated as responsible for NO production when the production of NOS-system appeared to be secondary (Shi and Li 2008). In contrast, Hong et al. (2008) made the conclusion that NR is unlikely to be the major generator of NO synthesized during the pathogen-triggered nitrosative burst. In addition, the levels of nitrate and nitrite were reported to be key determinants in NR-induced production of NO and that the NR activity in roots is lower than in other plant organs (Leleu and Vuylsteker 2004). Furthermore, significant NO production from NR is dependent upon high levels of nitrite and plants may not always have access to an abundant pool of nitrite, under which conditions NO production would be compromised (Hong et al. 2008).

The NR activity in tomato-nematode interactions was found to be higher in uninfected than in infected roots. NR activity decreased as the infection time increased. Given that nitrate is a substrate for NR-catalysed NO production, lowering of nitrate uptake in parallel with the NR activity during nematode infection, seems to suggest that NO production is also dependent on nitrate concentration, but roots challenged by nematodes have a reduced capacity in ensuring nitrate availability. Nevertheless, our data showed that NO production was reduced by NaN_3 (Table 1), suggesting that NR may be involved in nematode-induced NO. NR is known to be regulated by signals at the transcriptional or post-translational level, and mRNA level of NR genes, as well as NR protein accumulation, are reported to fluctuate in tomato roots (Jin et al. 2009). This could be the case in tomato-nematode interaction and further studies will be carried out to support this hypothesis. At the present, our findings suggest that NO involved in the defence signalling pathway, as well as in mediating the adaptive compatible response, is mainly produced by a NOS-like activity similarly to other plant-pathogen interactions (Zeidler et al. 2004).

The different patterns of ROS and H_2O_2 in incompatible and compatible interactions suggest that the first 24 h are critical for determining the plant response to invading nematodes (Melillo et al. 2006). Our studies showed in the incompatible interaction, when the juvenile is detected and defence response including cell death is induced, the initial (at 12 h) and rapid accumulation of both H_2O_2 and $O_2^{\cdot -}$ is followed by a prolonged oxidative burst in the host cells (at 24 and 48 h). Moreover, the high level of H_2O_2 produced during HR in the incompatible interaction suggests its direct role as an antimicrobial agent. In the compatible interaction, the first peaks of H_2O_2 and $O_2^{\cdot -}$ only occurring at 12 h after nematode infection, confirm that ROS not only act as causal triggers for HR but also activate genes encoding enzymes that prevent cells from oxidative damage (Apel and Hirt 2004). The detailed time course of $O_2^{\cdot -}$ formation confirmed that the most significant superoxide production is related to incompatible tomato-nematode relationship. The initial $O_2^{\cdot -}$ production at 12 h after nematode inoculation was followed by a significant increase in 24 h infected roots, when the parasites became sedentary and the onset of hypersensitive cell death started.

The temporal generation of signalling molecules ROS, in particular H_2O_2, and NO during nematode infection, is instrumental in initiating a cellular response. Furthermore, a direct interaction between NO and $O_2^{\cdot -}$ seems to be implicated in the production of the potent and versatile oxidant peroxynitrite, which might mediate the elicitor-induced cell death (Zeier et al. 2004).

Analyses for cell viability suggest a relationship between high Evan's blue uptake in tomato-avr infected roots and the oxidative burst. This can be explained by the specific necrotic spots in the roots, where presence of ROS has also been reported (Melillo et al. 2006). The analysis of DNA fragmentation did not show any clear laddering and this seems to confirm that PCD involves only few rows of cells. As reported for other plant-pathogen interactions (Tada et al. 2004), the reaction of

intracellular NO with $O_2^{\cdot-}$ which produces accumulation of H_2O_2 or generation of $ONOO^-$ strongly suggests that NO, $O_2^{\cdot-}$, H_2O_2, and $ONOO^-$ may be co-generated in cells directly injured by nematodes and undergoing to HR. In agreement with this, cell death in avr-infected roots increased sharply 24 and 48 h post-nematode inoculation, when large spots of necrotic cells were detected. These results suggest that NO and related reaction with other molecules can be differently perceived by neighbouring cells because of the relatively restricted diffusion of gaseous NO between the cells (Neill et al. 2008).

The present study reveals a defence mechanism that has not been previously described in tomato-nematode interaction and provides new insight into the complex regulation of ROS and NO metabolism by avr- and vir- RKN pathotypes in host roots. Accumulation of NO might be associated with the primary defensive response, serving as a second messenger in the signalling pathway of nematode attack. As plant growth regulators can be manipulated by nematodes as well as other pathogens, this suggests that developmental and defence signalling networks are interconnected. In conclusion, taking into account that the relationship between host and root knot nematodes is a quite complex and sophisticated mechanism, ROS and NO may act, both synergistically and independently, in plant immune response and may interrelate to form an oxidative cell death depending on the ability of the host to modulate a complex interacting signalling network for its defence. A deeper knowledge in determining the role of signal transduction pathway in tomato nematode-interactions should allow the development of alternative strategies for effective and safe plant parasite control.

Acknowledgments The authors thank Mr. Roberto Lerario for his helpful assistance with Figures. This work was supported by COST Action 872 "Exploiting genomics to understand plant-nematode interactions".

References

Abad, P., Favery, B., Rosso, M. N., & Castagnone-Sereno, P. (2003). Root-knot nematode parasitism and host response: molecular basis of a sophisticated interaction. *Molecular Plant Pathology, 4*, 217–224.

Apel, K., & Hirt, H. (2004). Reactive oxygen species: metabolism, oxidative stress, and signal transduction. *Annual Review of Plant Biology, 55*, 373–399.

Asai, S., Ohta, K., & Yoshioka, H. (2008). MAPK signalling regulates nitric oxide and NADPH oxidase-dependent oxidative bursts in *Nicotiana benthamiana*. *The Plant Cell, 20*, 1390–1406.

Bellafiore, S., Shen, Z., Rosso, M. N., Abad, P., Shih, P., & Briggs, S. P. (2008). Direct identification of the *Meloidogyne incognita* secretome reveals proteins with host cell reprogramming potential. *PLoS Pathogens, 4*, 1–12.

Corpas, F. J., Palma, J. M., del Río, L. A., & Barroso, J. B. (2009). Evidence supporting the existence of L-arginine dependent nitric oxide synthase activity in plants. *The New Phytologist, 184*, 9–14.

Courtois, C., Besson, A., Dahan, J., Bourque, S., Dobrowolska, G., Pugin, A., et al. (2008). Nitric oxide signalling in plants: interplays with Ca^{2+} and protein kinases. *Journal of Experimental Botany, 59*, 155–163.

Crawford, N. M., Galli, M., Tischner, R., Heimer, Y. M., Okamoto, M., & Mack, A. (2006). Response to Zemojtel et al: plant nitric oxide synthase: back to square one. *Trends in Plant Science, 11*, 526–527.

Delledonne, M., Zeier, J., Marocco, A., & Lamb, C. (2001). Signal interaction between nitric oxide and reactive oxygen intermediates in the plant hypersensitive disease resistance response. *Proceedings of the National Academy of Science of the USA, 98*, 13454–13459.

Du, S., Zhang, Y., Lin, X., Wang, Y., & Tang, C. (2008). Regulation of nitrate reductase by nitric oxide in Chinese cabbage pakchoi (*Brassica Chinensis* L.). *Plant Cell and Environment, 31*, 195–204.

Hong, J. K., Yun, B. W., Kang, J. G., Raja, M. U., Kwon, E., Sorhagen, K., et al. (2008). Nitric oxide function and signalling in plant disease resistance. *Journal of Experimental Botany, 59*, 147–154.

Jin, C. W., Du, S. T., Zhang, Y. S., Lin, X. Y., & Tang, C. X. (2009). Differential regulatory role of nitric oxide in mediating nitrate reductase activity in roots of tomato (*Solanum lycocarpum*). *Annals of Botany, 104*, 9–17.

Jones, J. D. G., & Dangl, J. L. (2006). The plant immune system. *Nature, 444*, 323–329.

Leleu, O., & Vuylsteker, C. (2004). Unusual regulatory nitrate reductase activity in cotyledons of *Brassica napus* seedlings: enhancement of nitrate reductase activity by ammonium supply. *Journal of Experimental Botany, 55*, 815–823.

Lum, H. K., Butt, Y. K. C., & Lo, S. C. L. (2002). Hydrogen peroxide induces a rapid production of nitric oxide in Mung Bean (*Phaseolus aureus*). *Nitric Oxide: Biology and Chemistry, 6*, 205–213.

Melillo, M. T., Bleve-Zacheo, T., Zacheo, G., & Gahan, P. B. (1989). Histochemical localisation of carboxyl esterases in roots of *Lycopersicon esculentum* in response to *Meloidogyne incognita* infection. *The Annals of Applied Biology, 114*, 325–330.

Melillo, M. T., Leonetti, P., Bongiovanni, M., Castagnone-Sereno, P., & Bleve-Zacheo, T. (2006). Modulation of ROS activities and H_2O_2 accumulation during compatible and incompatible tomato/root-knot nematode interactions. *The New Phytologist, 170*, 501–512.

Modolo, L. V., Augusto, O., Almeida, I. M. G., Pinto-Maglio, C. A. F., Oliveira, H. C., Seligman, K., et al. (2006). Decreased arginine and nitrite levels in nitrate reductase-deficient *Arabidopsis thaliana* plants impair nitric oxide

synthesis and the hypersensitive response to *Pseudomonas syringae*. *Plant Science, 171*, 34–40.

Neill, S. J., Bright, J., Desikan, R., Hancock, J. T., Harrison, J. T., & Wilson, I. (2008). Nitric oxide evolution and perception. *Journal of Experimental Botany, 59*, 25–35.

Requena, M. E., Egea-Gilabert, C., & Candela, M. E. (2005). Nitric oxide generation during the interaction with *Phytophthora capsici* of two *Capsicum annuum* varieties showing different degrees of sensitivity. *Physiologia Plantarum, 124*, 50–60.

Romero-Puertas, M. C., Rodriguez-Serrano, M., Corpas, F. I., Gomez, M., Del Rio, L. A., & Sandali, L. M. (2004). Cadmium-induced subcellular accumulation of $O_2^{\cdot-}$ and H_2O_2 in pea leaves. *Plant, Cell & Environment, 27*, 1122–1134.

Sagi, M., & Fluhr, R. (2006). Production of reactive oxygen species by plant NADPH oxidases. *Plant Physiology, 141*, 336–340.

Shi, F. M., & Li, Y. Z. (2008). *Verticillium dahliae* toxins-induced nitric oxide production in *Arabidopsis* is major dependent on nitrate reductase. *Biochemistry and Molecular Biology Reports, 41*, 79–85.

Tada, Y., Mori, T., Shinogi, T., Yao, N., Takahashi, S., Betsuyaku, S., et al. (2004). Nitric oxide and reactive oxygen species do not elicit cell death but induce apoptosis in the adjacent cells during the defense response of oat. *Molecular Plant-Microbe Interactions, 17*, 245–253.

Torres, M. A., Jones, J. D. G., & Dangl, J. L. (2006). Reactive oxygen species signalling in response to pathogens. *Plant Physiology, 141*, 373–378.

Van Breusegem, F., & Dat, J. F. (2006). Reactive oxygen species in plant cell death. *Plant Physiology, 141*, 384–390.

Wendehenne, D., Durner, J., & Klessig, D. F. (2004). Nitric oxide: a new player in plant signalling and defence. *Current Opinion in Plant Biology, 7*, 449–455.

Williamson, V. M., & Gleason, C. A. (2003). Plant-nematode interactions. *Current Opinion in Plant Biology, 6*, 327–333.

Yamamoto, A., Katou, S., Yoshioka, H., Doke, N., & Kawakita, K. (2006). Nitrate reductase is responsible for elicitin-induced nitric oxide production in *Nicotiana benthamiana*. *Plant & Cell Physiology, 47*, 726–735.

Zeidler, D., Zahringer, U., Gerber, I., Dubery, I., Hartung, T., Bors, W., et al. (2004). Innate immunity in *Arabidopsis thaliana*: liposaccharides activate nitric oxide synthase (NOS) and induce defense genes. *Proceedings of the National Academy of Science of the USA, 101*, 15811–15816.

Zeier, J., Delledonne, M., Mishna, T., Severi, E., Sonoda, M., & Lamb, C. (2004). Genetic elucidation of nitric oxide signalling in incompatible plant-pathogen interactions. *Plant Physiology, 136*, 2875–2886.